International Journal of Heat and Technology
Vol. 43, No. 1, February, 2025, pp. 85-92
Journal homepage: http://iieta.org/journals/ijht

Theoretical Analysis of LiBr-Water Absorption Air Condition Powered by Heated Pipe Evacuated Tube Solar Collector

Sanaa M. Hadi*, Mushtaq I. Hasan

Mechanical Engineering Department, College of Engineering, University of Thi-Qar, Thi-Qar 64001, Iraq

Corresponding Author Email: Sana.m@utq.edu.iq

https://doi.org/10.18280/ijht.430110

Received: 13 October 2024
Revised: 2 December 2024
Accepted: 17 December 2024
Available online: 28 February 2025

Keywords:
solar absorption refrigeration, absorption chiller, air conditioning, LiBr absorption cycle, solar LiBr air condition

ABSTRACT

The energy requirements of air conditioning systems are increasing over time. The use of solar absorption air conditioner can mitigate energy loss and reduce CO_2 emissions and the need to allocate such systems is very important. In this study, a thermodynamic analysis was performed by EES software for a single-effect solar-powered absorption chiller system with a 1 kW capacity, a heat pipe evacuated tube collector was used in Nasiriyah, Iraq. In the proposed system, the temperature of the (condenser, absorber, generator, and evaporator) were assumed to be (85℃, 38℃, 37℃, 5℃) respectively and the assumed heat exchanger efficiency was 0.5% and the working pair used was lithium bromide-water solution with variable concentrations according to the change of factors for each case studied where the generator contained the strong solution (rich in lithium bromide) and the absorber contained the weak solution. The findings have shown that the absorption refrigeration cycle's (coefficient of performance) rises as the temperature of the generator and evaporator rises and progressively falls as the temperature of the absorber and condenser rises. The maximum (COP) of 0.7 was attained when the generator temperature was 100℃ and the heat exchanger efficiency was 0.5; COP 0.77 was attained when the generator temperature was 95℃ and the heat exchanger efficiency was 80%. Furthermore, the heat exchanger's efficiency greatly boosted the performance coefficient by increasing the system efficiency.

1. INTRODUCTION

Finding effective and environmentally friendly air conditioning technology has become crucial due to growing concerns about energy usage, environmental impact, and the need for sustainable solutions. A building's interior temperature may be impacted by heat loads, solar radiation, internal heat sources. Indoor temperatures that exceed the acceptable range can cause a multitude of health problems for residents as well as a noticeable drop in productivity. Numerous passive and active methods may be used to reduce the harmful effects of indoor heating. The passive cooling method disperses excess heat in naturally occurring sinks like the ground, the air, or a structure's thermal mass. The cooling requirements of a structure can be affected by both passive and natural means, passive approaches, however, are unable to address all climatic conditions and satisfy interior comfort needs. In order to regulate the interior temperature, humidity level, and occupants' comfort level, mechanical cooling can be necessary. Up until 1955, just around 2% of homes in the USA had mechanical cooling systems installed. Nonetheless, economic growth is what drove the air conditioner (AC) market's expansion between 1950 and 1980. By 1990, air conditioning systems were installed in about 50% of US homes. Conventional air conditioning systems utilise a lot of electricity produced from fossil fuels, which increases greenhouse gas emissions and the world's energy crisis. A viable approach that provides a renewable and sustainable alternative is the integration of solar power into air conditioning units [1]. Scientists have been working to create sustainable and contemporary cooling systems using sources of renewable energy, particularly solar energy, which is clean, limitless, and abundant, in order to address the issues raised by current air conditioning systems [2]. More energy is being utilised for thermal comfort than for any other energy service, and this growth is occurring more quickly than for any other energy service. According to a recent report by the International Energy Agency (IEA), buildings account for 20% of global electricity consumption used for cooling. Furthermore, according to the report, about two thirds of homes worldwide could have air conditioning by 2050. Thus, by 2050, the energy required for thermal comfort will triple [3]. Therefore, in order to comply with new environmental regulations and minimise energy consumption for thermal comfort, innovative techniques for cooling and heating systems based on renewable energy sources are imperative [4]. Considering the close relationship between the quantity of renewable energy sources (solar, wind) and the energy needed for space cooling, these studies are regarded as a compelling choice. It is therefore possible to meet this requirement by using solar and wind energy [5]. For solar cooling applications, absorption technology makes the most sense [6-

8]. Nonetheless, LiBr–H_2O is frequently employed in absorption cooling systems as a working fluid. LiBr–H_2O has been a commonly used absorption material in air conditioning systems since the late 1960s [9, 10]. The 1980s saw it develop into a dependable and effective method using thermal energy [9]. These days, the best substitutes for creating chilled water for cooling and space use are LiBr–H_2O absorption chillers, which work by putting hot water into their generator. One of the earliest and most important evaporation systems for food storage, air conditioning, refrigeration, and chilled water applications is the Vapour Absorption Refrigeration System (VARS) [11]. Additionally, VARS is thought to be a potent remedy that could lessen the major issues affecting human life everywhere, like pollution and the energy and water crises [12]. The most prevalent couples are LiBr–H_2O and NH_3–H_2O, working fluids in VARS [12, 13]. The two most widely used types of solar collectors are evacuated tube collectors (ETC) and flat plate collectors (FPC). ETC is used to raise the temperature and is more effective in bleak and chilly conditions [14, 15]. There are many research in literature studied absorption air condition such as: Ketjoy and Mansiri [16] looked at the LiBr–H_2O performance of chiller with a (35 kW) cooling capacity, (72 m^2) of ETC, and an auxiliary boiler. Porumb et al. [17] studied, the experimental and numerical investigations, the COP values were, respectively, 0.691 and 0.73. There was a 5.48% discrepancy. This indicates that the numerical model is workable and may closely resemble the findings of the actual investigation for this application. Martínez et al. [18] conducted an experimental and theoretical investigation on a LiBr–H_2O single effect absorption chiller. It has a 55 kW cooling capacity and was powered by ETC. The findings showed that a COP value of 0.69 was attained and that the cooled water was generated at a temperature of 7℃, while the maximum generator temperature did not rise over 100℃. In this paper the LiBr-water air condition combined with solar energy has been studied in the climate of Nasiria city, south of Iraq. A heated pipe evacuated tube solar collector has been used as a heat source.

2. THERMODYNAMIC MODELING

2.1 System description

The core parts of the absorption system are the generator, evaporator, absorber, condenser, expansion valve, pump, and solution heat exchanger. as seen in Figure 1, where the primary absorption components refrigeration cycle is the principle of operation of the cycle: The hot water coming from the solar collector enters the generator where it separates the lithium bromide from the water because the boiling point of lithium bromide is lower than that of water, which leads to the evaporation of the water and the steam goes to the condenser (7) where it has a high temperature and pressure. As for the LiBr that separated from the water, it considered a weak solution it moves to the heat exchanger (4) so that the exchanger reduces its temperature so that enters the absorber after passing through the expansion valve to reduce its pressure (6). The water vapor after entering the condenser is cooled to condense and exits the condenser (8) as a liquid at a low temperature to enter the evaporator after passing through the capillary tube that reduces the temperature and pressure of the water. The refrigerant liquid evaporates in the evaporator to absorbs heat from cooling medium go to the absorber as low-pressure vapor (10) to mix with the strong solution. After that, the strong solution (1) moves through the pump (2) to enter the heat exchanger where it raises its temperature to enter the generator (3) as a strong solution. Then the cycle is repeated again because the cycle here is a closed single-effect cycle.

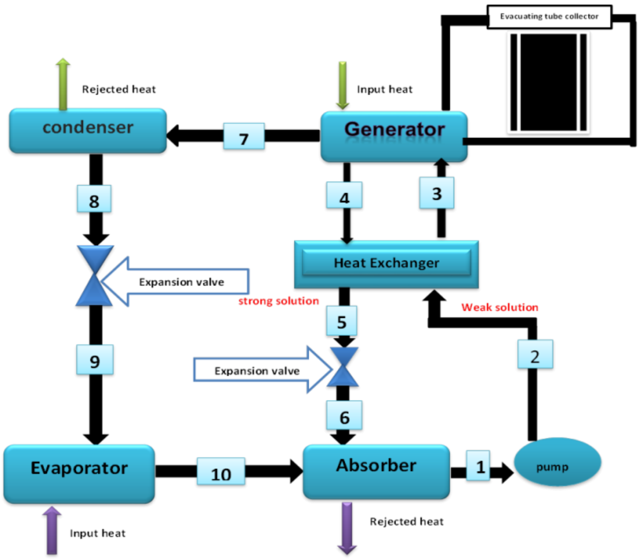

Figure 1. The basic components of the absorption air-conditioning system

2.2 Assumptions

1- A cooling capacity at evaporator is 1 KW.
2- Pressure drop there is no in the pipes.
3- The pump work is negligible.
4- The solution pump's efficiency is 0.5.
5- Frictional losses are negligible.
6- Pumping process is isentropic.
7- Saturated Liquid refrigerant leaving the condenser.
8- Saturated water refrigerant vapor out the evaporator.

2.3 Governing equations

The basic single effect LiBr-water absorption chiller only requires the condenser, evaporator, generator, absorber, and solution heat exchanger. Other required parts include the solution pump and valves. These components' mass and energy balances are as follows:

At the evaporator:

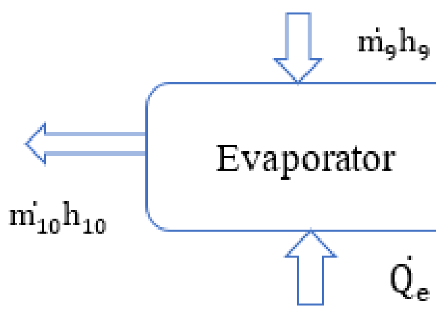

$$\dot{m_9} = \dot{m_{10}} = \dot{m_{ref}} \tag{1}$$

$$\dot{Q}_e = \dot{m_{ref}}(h_{10} - h_9) \tag{2}$$

$$\dot{m}_{ref} = \frac{\dot{Q}_e}{(h_{10} - h_9)} \tag{3}$$

Circulation ratio is calculated by dividing the mass flow rate of the working fluid by the mass flow rate of the solution via the pump [19].

$$F_r = \frac{X_{ss}}{X_{ss} - X_{ws}} \tag{4}$$

$$\dot{m}_{ss} = \dot{m}_{ref} F_r \tag{5}$$

$$\dot{m}_{ws} = \dot{m}_{ss} + \dot{m}_{ref} \tag{6}$$

$$\therefore \ \dot{m}_{ws} = \dot{m}_{ref}(F_r - 1) \tag{7}$$

At the absorber:

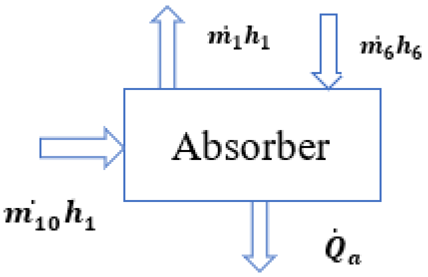

$$\begin{gathered} \dot{m}_1 h_1 + Q_a = \dot{m}_6 h_6 + \dot{m}_{10} h_{10} \\ \dot{m}_6 = \dot{m}_{ss} \\ \dot{m}_{10} = \dot{m}_{ref} \\ \dot{m}_1 = \dot{m}_{ws} \end{gathered} \tag{8}$$

$$\dot{m}_{ws} h_1 + Q_a = \dot{m}_{ss} h_6 + \dot{m}_{ref} h_{10} \tag{9}$$

$$Q_a = \dot{m}_6 h_6 + \dot{m}_{10} h_{10} - \dot{m}_1 h_1 \tag{10}$$

where,

$$\begin{gathered} h_1 = h_2 = enthalpy\ at\ (T_1 = T_a\,, X_{ws}) \\ h_5 = h_6 = enthalpy\ \ at\ (T = T_5, X_{ss}) \\ *\ throttling\ proccess \\ h_{10} = enthalpy\ at\ (T_{10} = T_E\,) \end{gathered}$$

At the heat exchanger:

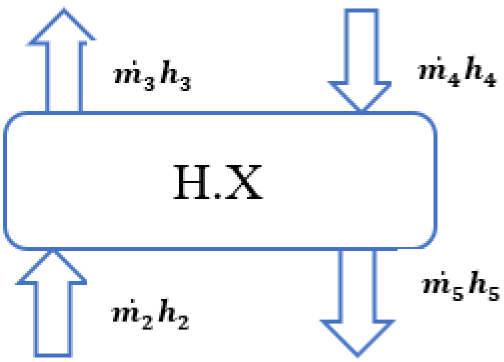

$$\dot{m}_2 = \dot{m}_3 = \dot{m}_{ws} \tag{11}$$

$$\dot{m}_4 = \dot{m}_5 = \dot{m}_{ss} \tag{12}$$

$$\dot{m}_3 h_3 - \dot{m}_2 h_2 = \dot{m}_4 h_4 - \dot{m}_5 h_5 \tag{13}$$

Heat exchanger effectiveness is equal to:

$$Ef = \frac{(T_4 - T_5)}{(T_4 - T_2)} \tag{14}$$

Assuming Heat exchanger effectiveness is (0.5).
where,
T_5: Temperature of the strong solution exiting the absorber from the heat exchanger.

$$\therefore T_5 = 61°\mathrm{C}$$

$$T_3 = T_a + \left[E * \left(\frac{X_{ss}}{X_{ws}}\right) * \left(\frac{C_{ws}}{C_{ss}}\right) * (T_g - T_a)\right] \tag{15}$$

where,
T_3: Temperature of the weak solution exiting the generator from the heat exchanger.
C_{ss}: Specific heat of strong solution calculated by using following relation:

$$C_{ss} = 4.184 * \left(1.01 - 1.23\,X_{ss} + 0.48\,{X_{ss}}^2\right) \tag{16}$$

C_{ws}: Specific heat of weak solution can calculated by using following relation:

$$\begin{gathered} C_{ws}: 4.184 * \left(1.01 - 1.23\,X_{ws} + 0.48\,{X_{ws}}^2\right) \\ \therefore T_3 = 63.4 \\ Q_{shx} = m_{ws}(h_3 - h_2) = m_{ss}(h_4 - h_5) \end{gathered} \tag{17}$$

At the generator:

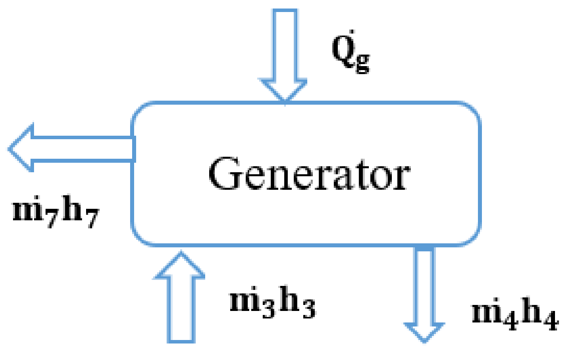

$$\dot{Q}_g + \dot{m}_3 h_3 = \dot{m}_7 h_7 + \dot{m}_4 h_4 \tag{18}$$

$$\dot{m}_3 = \dot{m}_{ws} \quad , \dot{m}_4 = \dot{m}_{ss} \quad , \dot{m}_7 = \dot{m}_{ref} \tag{19}$$

$$\therefore \ \dot{Q}_g = \dot{m}_7 h_7 + \dot{m}_4 h_4 - \dot{m}_3 h_3 \tag{20}$$

At the condenser:

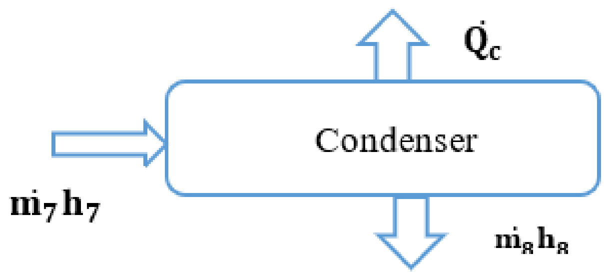

$$\dot{Q}_c + \dot{m}_8 h_8 = \dot{m}_7 h_7 \tag{21}$$

$$\dot{m}_8 = \dot{m}_7 = \dot{m}_{ref} \tag{22}$$

$$\therefore \dot{Q}_c = \dot{m}_{ref}(h_7 - h_8) \tag{23}$$

The expansion valves:

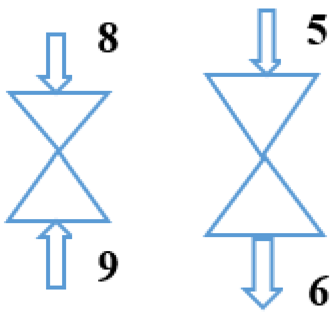

$$\dot{m}_5 = \dot{m}_6 = \dot{m}_{ref} \tag{24}$$

$$h_5 = h_6 \tag{25}$$

$$\begin{gathered} \dot{m}_8 = \dot{m}_9 = \dot{m}_{ref} \\ h_8 = h_9 \end{gathered} \tag{26}$$

At the pump:

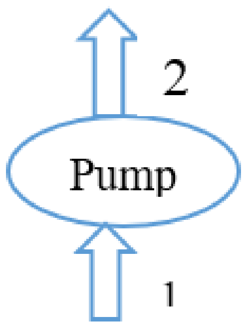

$$\dot{m}_1 = \dot{m}_2 = \dot{m}_{ws} \tag{27}$$

$$W_p = \dot{m}_{ws}(h_2 - h_1) \tag{28}$$

Performance Coefficient (COP)

The following formula is used to determine the absorption refrigeration cycle's coefficient of performance:

$$\mathrm{COP} = \frac{\dot{Q}_e}{W_p + \dot{Q}_g} \tag{29}$$

Work of pump is negligible:

$$\therefore \mathrm{COP} = \frac{\dot{Q}_e}{\dot{Q}_g} \tag{30}$$

3. SOLAR COLLECTOR

A solar assisted refrigeration system the solar collector considered as one of its essential components, converts solar collector considered as one of its essential components, converts solar energy into thermal energy, which in turn powers the absorption chiller [20]. Collectors made of evacuated tubes capture solar heat. Water was chosen as the heat transfer fluid for the solar array due to its excellent thermal conductivity and heat capacity. The water that flows through the ETC collectors is subsequently warmed by the heat generated by solar thermal energy [21]. The cycle begins when the target temperature is attained. Due to energy losses along the heat-transfer process from the absorbent to the tubes, the amount of heat absorbed does not equal the amount of heat that is actually transferred to the heat transfer liquid. The generator needs the usable heat that the solar collector collects as an input during the absorption cycle Equation provides the collector's thermal efficiency:

$$\eta_c = \eta + a_1 \frac{\Delta T}{I_T} - a_2 \frac{(\Delta T)^2}{I_T} \tag{31}$$

where:

ΔT: The variance between the ambient temperature Ta and the average water temperature through the solar collector Tm.

I_T: The entire amount of radiation that struck the absorber surface.

η: is the optical efficiency.

a_1 and a_2: Loss coefficients.

4. THE SOFTWARE FOR ENGINEERING EQUATION SOLVING (EES)

All of the modelling and analysis, the Engineering Equation Solver (EES) programme, developed by FCHART SOFTWARE®, is used for this investigation. The EES software package combines the programming frameworks of C++ and FORTRAN with graphical capabilities, numerical integration, and several other useful mathematical operations. It also covers the links between thermodynamics, iteration, and transport properties (of many widely encountered substances, including as air, water, and most refrigerants). These characteristics make the EES a very helpful tool for resolving fluid mechanics, thermodynamics, and heat transport issues. There are several technological uses for the ESS.

5. RESULTS AND DISCUSSION

5.1 Validation

The validity of the current numerical results was verified by comparing the results of the current study with the published results of Ketfi et al. [19] using the same problem geometry and conditions.

Figure 2 shows the connection between the generator temperature and the illustrates performance coefficient when the heat exchanger efficiency is (0.7) and the absorber, condenser, and evaporator's temperatures are (40°C, 40°C, 7°C) respectively. We note from the figure that the error percentage between the current results and the results of Ketfi et al. [19] is 2%.

Figure 3 shows the variation of evaporator temperature with coefficient performance when the heat exchanger efficiency is (0.7) and the temperature of absorber, condenser and evaporator are (40°C, 40°C, 7°C) respectively. The results of the present study showed agreement with the results of the Ketfi et al. [19] with 2% error rate.

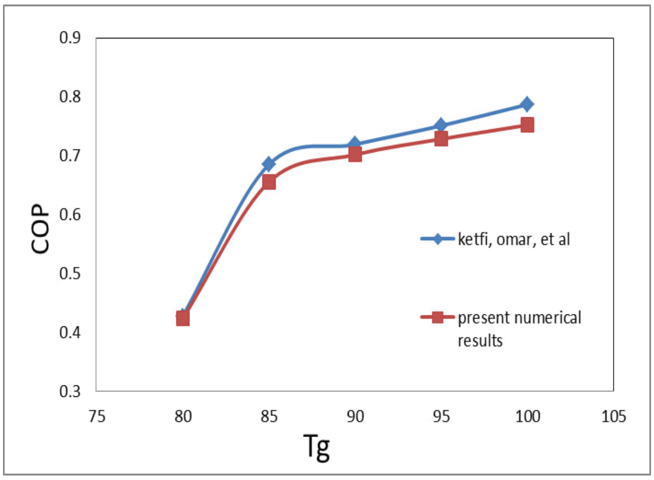

Figure 2. Validation of the present numerical model with published results of Ketfi et al. [19]

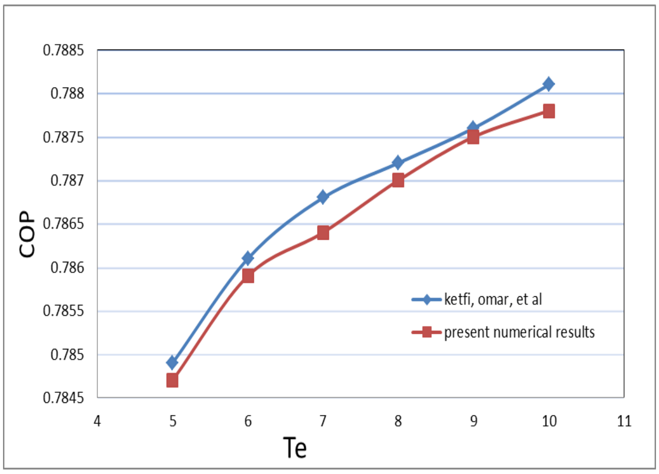

Figure 3. Validation of current numerical model with results that have been published of Ketfi et al. [19]

5.2 Results

Figure 4 illustrates how the condenser temperature and the coefficient of performance (COP) relate to each other for varying heat exchanger efficiency values while the evaporator's capacity is constant and the generator, absorber, and evaporator temperatures are 85℃, 37℃, and 5℃, respectively. When the condenser temperature rises concurrently with varying heat exchanger efficiency values, the coefficient of performance decreases. There are several explanations for this. The condenser in an absorption cooling system is in charge of rejecting heat from the refrigerant. Reduced heat rejection efficiency as the condenser temperature rises indicates that the refrigerant cannot condense as efficiently as needed, resulting in less efficient operation. An improved heat exchanger results in better heat transfer, lower energy inputs, and optimised system performance, all of which raise the coefficient of performance (COP) in cooling applications. A more efficient heat exchanger improves the heat transfer between the working fluid (refrigerant) and the heat source (or sink).

Figure 5 exhibits the connection between the condenser temperature and the coefficient of performance for varying generator temperature values when the heat exchanger efficiency is 50%, the evaporator's capacity is constant, and the absorber and evaporator temperatures are 37℃ and 5℃, respectively. If the condenser temperature rises and the generator temperature rises as well, the energy required to drive the absorption process rises. This can lead to increased thermal energy input without a proportional increase in cooling output, diminishing the COP. Increasing the condenser temperature usually results in higher pressures within the system. While higher pressures can enhance the efficiency of the generator and absorption processes, they can also reduce the vapor pressure differential needed for effective vaporization in the evaporator. As a result, the evaporator may struggle to maintain its cooling performance, which directly impacts COP.

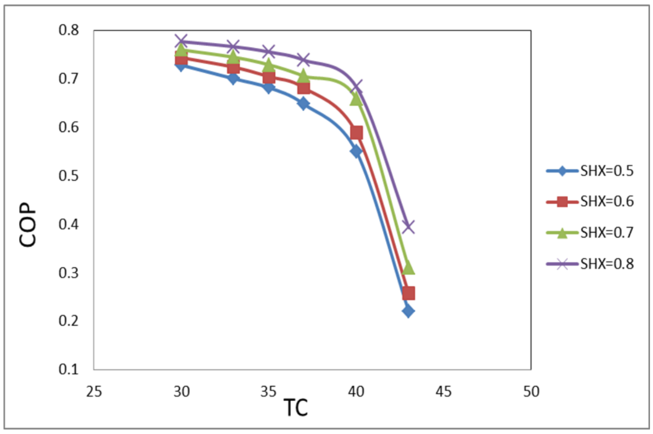

Figure 4. Change in the absorption cooling system's coefficient of performance (COP) with condenser temperature for varying heat exchanger efficiency levels

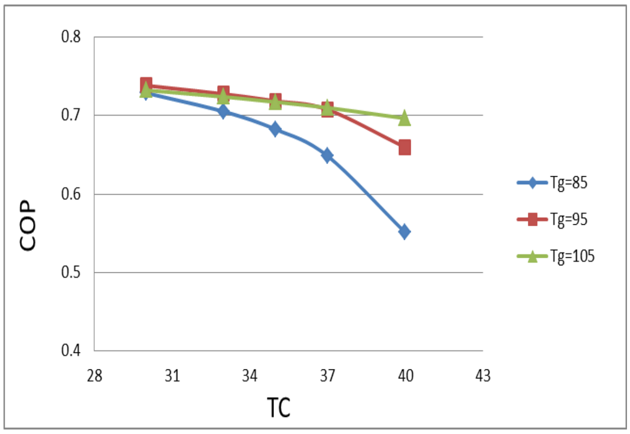

Figure 5. Variation between the COP and condenser temperature for different value of generator temperature

Figure 6 illustrates the relationship between the absorber temperature and the coefficient of performance for various heat exchanger efficiency values at ($T_g = 85℃, T_c = 38℃, T_e = 5℃$). This figure shows that improving the heat exchanger's efficiency is intended to improve the system's performance; nevertheless, high absorber temperatures may result in lower absorption efficiency and higher energy input. They all work together to lower the absorption refrigeration cycle's coefficient of performance.

Figure 7 variation of evaporator temperature (Te) with the coefficient performance for different value of heat exchanger efficiency when the capacity of system is constant (1 KW) and ($T_g = 85℃,\ T_a = 37℃,\ T_c = 38℃$) steady concentration of the weak solution in the generator and a decline in the absorber's strong solution concentration due to the generator's constant temperature result from raising the evaporator temperature when the temperature of the other system components and the system's cooling capacity remain constant. An increase in the performance factor results from this since less heat enters the system. A well-designed capacity proofing system, enhanced heat exchanger efficiency, and higher evaporator temperature may all greatly raise an absorption refrigeration cycle's coefficient of performance (COP). This rise is mostly the result of improved thermodynamic efficiency, less effort needs, and more efficient use of heat transfer processes.

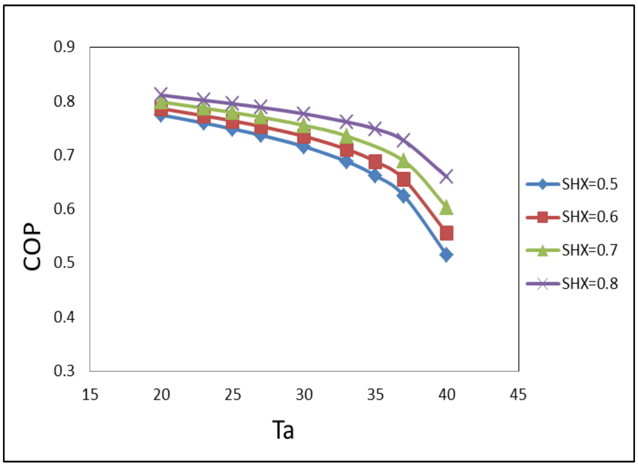

Figure 6. The (COP) for different heat exchanger efficiency levels in relation to absorber temperature

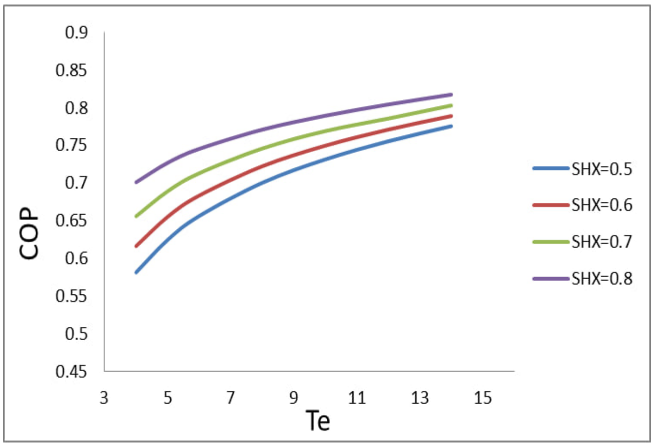

Figure 7. Variation between the COP and temperature of evaporator for different values of SHX

Figure 8 illustrates how the absorption cooling system's coefficient performance changes with generating temperatures for different heat exchanger efficiency values. The evaporator's capacity remains constant, while the temperatures of the condenser, absorber, and evaporator are 38°C, 37°C, and 5°C, respectively. By enhancing vapor output, vapor quality and pressure, and system performance, increasing the generator temperature raises the coefficient of performance (COP) in a solar-powered absorption refrigeration cycle with constant temperatures and system capacity. For the same energy input, these characteristics allow the system to provide its cooling effect more efficiently. The dynamic changes caused by increasing the generator temperature can therefore lead to a noticeable improvement in COP and eventually more effective refrigeration, even when the temperatures of the remainder of the cycle remain unchanged.

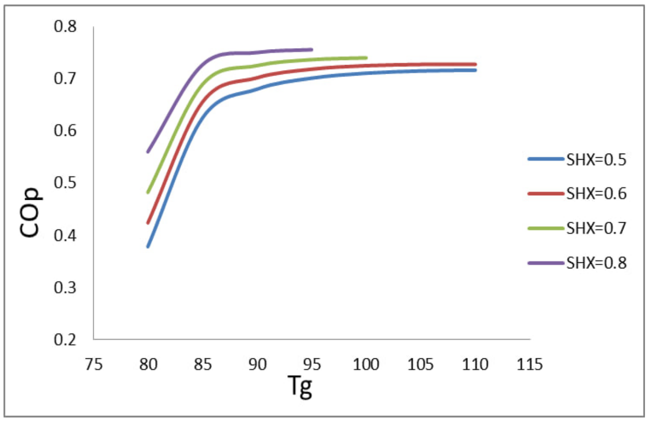

Figure 8. The COP of the absorption cooling system with generator temperatures for different values of heat exchanger efficiency

Figure 9 illustrates the relationship between the amount of heat produced by each component of the cooling system and the rise in the generator's temperature, assuming that the evaporator's heat is one kilowatt, the condenser's temperature is 38°C, the absorber's temperature is 37°C, and the evaporator's temperature is 5°C. When the generator's temperature rises, the refrigerant (often ammonia or a similar working fluid) begins to vaporize. The heat input initially causes rapid vaporization of the liquid refrigerant, which requires a significant amount of energy (latent heat). As the refrigerant vaporizes more efficiently at higher temperatures, the amount of heat entering the generator decreases rapidly because a larger portion of the energy is used for the phase change rather than raising the temperature. the generator's temperature continues to rise, the system may start reaching a thermodynamic equilibrium state where the amount of vaporization and condensation stabilizes. The balance between the heat entering the generator and the heat being lost (through various losses) affects the overall heat input. At this point, the need for additional heat to maintain high rates of vaporization decreases, hence the rate of absorption decreases more slowly. the rapid decrease in the amount of heat rejected by the absorber when the temperature of the generator increases is primarily due to the higher vapor pressures and absorption rates resulting from the increase in temperature, along with significant heat transfer efficiency due to favorable temperature gradients. As the system stabilizes and approaches thermodynamic equilibrium, the rate of heat rejection becomes slower and more stable, resulting in a gradual decline. Understanding these dynamics is crucial for optimizing the performance of absorption refrigeration cycles.

Figure 10 represents the relation between the system's COP and the heat exchanger's efficiency at various generator temperature values. In an absorption refrigeration cycle, the (COP) may indeed be positively impacted by improving the efficacy of the heat exchangers, especially when the generator temperature increases in an evacuated cycle. Better thermal contact and heat transmission enable the refrigerant to evaporator more fully and effectively when the generator temperature is raised in conjunction with efficient heat exchangers. As a result, more refrigerant vapor enters the absorber, increasing the refrigeration effect that the evaporator produces. When improving the effectiveness of the heat exchanger, a significant increase in the (COP) of the absorption refrigeration cycle can be achieved. This facilitates better energy utilization and reduces operational and environmental costs.

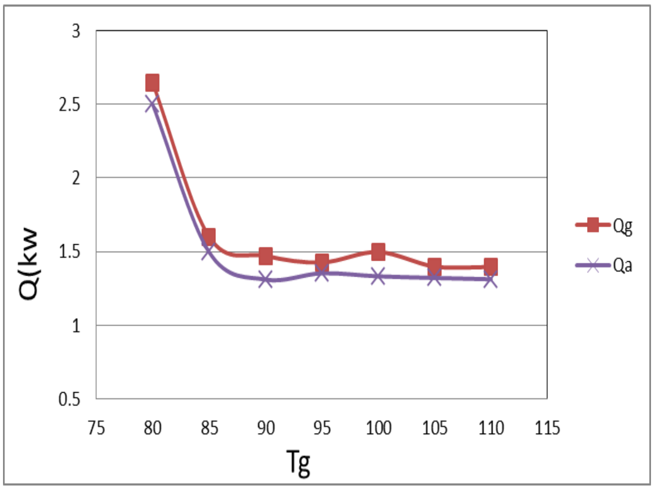

Figure 9. Variation of heat amount with generator temperatures

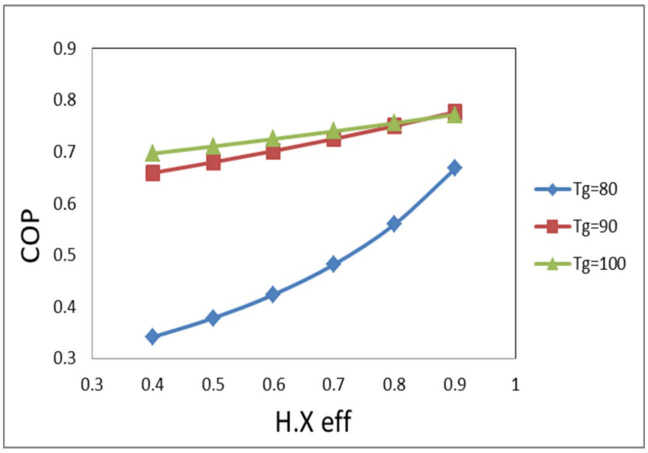

Figure 10. Variation of coefficient of performance with the efficiency of heat exchanger at different value of generator temperature

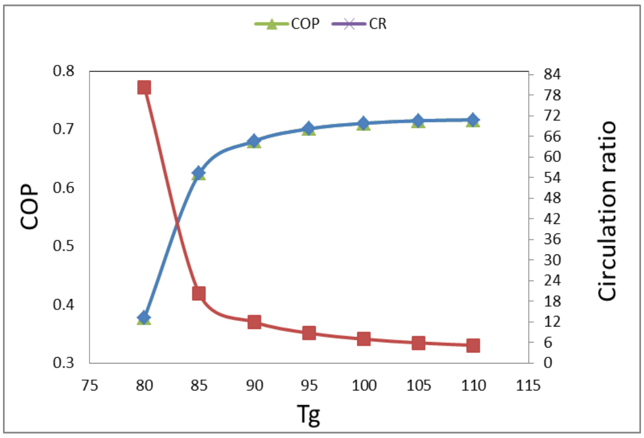

Figure 11. The variation of COP and the circulation ratio with generator temper

Figure 11 show how the temperature of the generator affects the COP and circulation ratio for lithium bromide-water $(\dot{m}_{ss}/\dot{m_{ref}})$ when the capacity of evaporator is 1KW and the condenser, absorber, and evaporator temperature are (38°C, 37°C, 5°C) respectively. The graphic illustrates how the circulation ratio falls and the increases coefficient of performance as the generator temperature rises. This is due to the fact that when the maximum generator temperature rises, so does the amount of LiBr-H_2O that evaporates. By definition, as the volume of refrigerated vapor increases, the circulation ratio will also decrease.

6. CONCLUSIONS

The most viable alternative for cooling systems in the future may be solar energy. A sensible solution to the increasing need for energy consumption is a solar absorption cooling system. This study examines a single-effect LiBr–H_2O absorption cooling system driven by solar thermal energy employing an ETC and a 1 kW cooling capacity using EES/Simulink technology, which is founded on the first rule of thermodynamics. First, this numerical model has been validated using experimental and theoretical data from the literature. Next, a range of cooling system cycle temperatures were used to evaluate the cycle's coefficient of performance (COP). The range (0.6 to 5.8%) represented the variation in COP values. Furthermore, the temperature at which the cycle may be run without was crystallization mated using this kind of model. And for the generator, it was 110°C.

The following summarises the important results of this work:

1. The most important factor on the results is the temperature of the generator. In this system, temperatures from 75°C to 110°C were used without crystallization.
2. The highest temperatures at which the cycle operates without crystallization of the generator, condenser, absorber and evaporator are (110°C, 43°C, 42°C, 16°C) respectively.
3. With a temperature of generator 95°C, the COP maximum value recorded was 0.77.
4. Heat exchanger efficiency and generator temperature rise, the coefficient of performance rises as well.
5. The temperature of the generator and evaporator raised the absorption refrigeration cycle's coefficient of performance, while the temperature of the absorber and condenser caused it to progressively drop.
6. As generator temperature and heat exchanger efficiency rise, so does the coefficient of performance.

REFERENCES

[1] Aridhi, E., Bemri, H., Mami, A. (2018). Solar air-conditioning systems. Sustainable Air Conditioning Systems. http://doi.org/10.5772/intechopen.72189

[2] Suman, S., Khan, M.K., Pathak, M. (2015). Performance enhancement of solar collectors—A review. Renewable and Sustainable Energy Reviews, 49: 192-210. https://doi.org/10.1016/j.rser.2015.04.087

[3] Birol, F.J.I.E.A. (2018). The future of cooling: opportunities for energy-efficient air conditioning. International Energy Agency, 526. https://doi.org/10.2867/67846

[4] She, X.H., Cong, L., Nie, B., Leng, G., Peng, H., Chen, Y., Zhang, X., Wen, T., Yang, H., Luo, Y. (2018). Energy-efficient and-economic technologies for air conditioning with vapor compression refrigeration: A

comprehensive review. Applied Energy, 232: 157-186. https://doi.org/10.1016/j.apenergy.2018.09.067

[5] Petela, K., Szlęk, A. (2016). Assesment of passive cooling in residential application under moderate climate conditions. Ecological Chemistry and Engineering, 23(2): 211-225. https://doi.org/10.2428/ecea.2016.23(2)16

[6] Mansouri, R. (2016). Theoretical and experimental study of absorption and absorption/diffusion refrigerating machines using ammonia as a refrigerant: simulation under steady-state and dynamic regimes and experimental characterization of a pilot. Universitat Rovira, Virgili.

[7] Abrudan, A.C., Pop, O.G., Serban, A., Balan, M.C. (2019). New perspective on performances and limits of solar fresh air cooling in different climatic conditions. Energies, 12(11): 2113. https://doi.org/10.3390/en12112113

[8] Khan, M.S., Abid, M., Bashir, M.A., Amber, K.P., Khanmohammadi, S., Yan, M. (2021). Thermodynamic and exergoeconomic analysis of a novel solar-assisted multigenerational system utilizing high temperature phase change material and hybrid nanofluid. Energy Conversion and Management, 236: 113948. https://doi.org/10.1016/j.enconman.2021.113948

[9] Wang, X., Chua, H.T. (2009). Absorption cooling: A review of lithium bromide-water chiller technologies. Recent Patents on Mechanical Engineering, 2(3): 193-213.

[10] Lazzarin, M.R. (2007). Solar cooling plants: How to arrange solar collectors, absorption chillers and the load. International Journal of Low-Carbon Technologies, 2(4): 376-390. https://doi.org/10.1093/ijlct/2.4.376

[11] Srikhirin, P., Aphornratana, S., Chungpaibulpatana, S. (2001). A review of absorption refrigeration technologies. Renewable and Sustainable Energy Reviews, 5(4): 343-372. https://doi.org/10.1016/S1364-0321(01)00003-X

[12] Wang, M., Becker, T.M., Schouten, B.A., Vlugt, T.J.H., Infante Ferreira, C.A. (2018). Ammonia/ionic liquid based double-effect vapor absorption refrigeration cycles driven by waste heat for cooling in fishing vessels. Energy Conversion and Management, 174: 824-843. https://doi.org/10.1016/j.enconman.2018.08.060

[13] Patel, H.A., Patel, L.N., Jani, D., Christian, A. (2016). Energetic analysis of single stage lithium bromide water absorption refrigeration system. Procedia Technology, 23: 488-495. https://doi.org/10.1016/j.protcy.2016.03.054

[14] Ghoneim, A.A., Shabana, H.M., Shaaban, M.S., Mohammedein, A. (2016). Performance analysis of evacuated tube collector in hot climate. European International Journal of Science and Technology, 5(3): 8-20.

[15] Abid, M., Khan, M.S., Ratlamwala, T.A.H., Malik, M.N., Ali, H.M., Cheok, Q. (2021). Thermodynamic analysis and comparison of different absorption cycles driven by evacuated tube solar collector utilizing hybrid nanofluids. Energy Conversion and Management, 246: 114673. https://doi.org/10.1016/j.enconman.2021.114673

[16] Ketjoy, N., Mansiri, K. (2013). Performance evaluation of 35 kW LiBr–H_2O solar absorption cooling system in Thailand. Energy Procedia, 34: 198-210. https://doi.org/10.1016/j.egypro.2013.06.748

[17] Porumb, R., Porumb, B., Balan, M. (2017). Numerical investigation on solar absorption chiller with LiBr-H2O operating conditions and performances. Energy Procedia, 112: 108-117. https://doi.org/10.1016/j.egypro.2017.03.1071

[18] Martínez, P.J., Martínez, J.C., Lucas, M. (2012). Design and test results of a low-capacity solar cooling system in Alicante (Spain). Sol. Energy, 86(10): 2950-2960. https://doi.org/10.1016/j.solener.2012.06.030

[19] Ketfi, O., Merzouk, M., Merzouk, N.K., El Metenani, S. (2015). Performance of a single effect solar absorption cooling system (Libr-H_2O). Energy Procedia, 74: 130-138. https://doi.org/10.1016/j.egypro.2015.07.534

[20] Henning, H.M. (2007). Solar assisted air conditioning of buildings – an overview. Applied Thermal Engineering, 27(10): 1734-1749. https://doi.org/10.1016/j.applthermaleng.2006.07.021

[21] Sanchita Singh, Pushpendra Singh. (2023). Mathematical modeling and performance analysis of a solar assisted vapour absorption refrigeration system. E3S Web of Conferences, 405: 02009. https://doi.org/10.1051/e3sconf/202340502009